



CHORUS

This is the accepted manuscript made available via CHORUS. The article has been published as:

Model of the cooperative rearranging region for polyhydric alcohols

Masahiro Nakanishi (□□□□) and Ryusuke Nozaki (□□□□)

Phys. Rev. E **84**, 011503 — Published 19 July 2011

DOI: [10.1103/PhysRevE.84.011503](https://doi.org/10.1103/PhysRevE.84.011503)

Model of Cooperative Rearranging Region for Polyhydric Alcohols

Masahiro Nakanishi (中西真大) and Ryusuke Nozaki (野寄龍介)

Department of Physics, Faculty of Science, Hokkaido University, Sapporo, Hokkaido 060-0810, Japan

Abstract

A simplified model of a hydrogen-bonding network is proposed in order to clarify the microscopic structure of cooperative rearranging region (CRR) in Adam-Gibbs theory [G. Adam and J. H. Gibbs, *J. Chem. Phys.* 43, 139 (1965)]. Our model can be solved analytically, and it successfully explains the reported systematic features of the glass transition of polyhydric alcohols. In this model, hydrogen bonding is formulated based on binding free energy. Assuming a cluster of molecules connected by double hydrogen bonds is a CRR, and approximating the hydrogen-bonding network as a Bethe lattice in percolation theory, the temperature dependence of the structural relaxation time can be obtained analytically. Reported data on relaxation time are well described by the obtained equation. By taking the lower limit of binding free energy with this equation, the Vogel-Fulcher-Tammann equation can be derived. Consequently, the fragility index and glass transition temperature can be expressed as functions of the number of OH groups in a molecule, and this relation agrees well with the reported experimental data.

1. Introduction

Some hydrogen-bonding liquids are well-known glass-forming liquids. Despite their simple molecular structure, hydrogen-bonding liquids (especially polyhydric alcohols) often maintain a supercooled state without crystallization, and consequently a variety of materials are available for studies on glass transition. For this reason, hydrogen-bonding liquids can sometimes enable systematic study based on differences in molecular structure; actually, they have long been used in studies on glass transition [1-9]. Interesting systematic features of the glass transition of polyhydric alcohols have been revealed through recent experimental studies [3-9], the results of which should inspire new theoretical approaches to studying the glass transition of hydrogen-bonding liquids.

Sugar alcohols are one type of polyhydric alcohol and generally consist of a linear

carbon backbone with an equal number of OH groups and C atoms ($N_{OH} = N_C$): for example, glycerol ($N_{OH} = N_C=3$), threitol ($N_{OH} = N_C=4$), xylitol ($N_{OH} = N_C=5$), and sorbitol ($N_{OH} = N_C=6$). By using this series of materials, Döb et al. and Minoguchi et al. have found systematic features in the glass transition of these materials. In particular, the temperature dependence of structural α -relaxation time (or frequency) changes systematically against N_{OH} or N_C , or both. Consequently, the fragility index (m) [10] and the glass transition temperature (T_g) show systematic dependence on these parameters [3-7]. In these previous studies, however, no distinction was made between the parameters N_{OH} and N_C . To reveal which parameter more strongly affects the glass transition, in our previous works we experimentally investigated a series of trihydric alcohols ($N_C \neq N_{OH} = 3$) [8, 9]. We found that N_{OH} is more dominant than N_C and that the probability of hydrogen bond formation is similar among a variety of polyhydric alcohols regardless of differences in their molecular structures (position of OH, branching of the carbon chain, etc.).

Generally, systematic features imply a simple physical mechanism. From the above experimental results, the glass transition behavior of polyhydric alcohols can be explained by a model that is much simpler than the actual molecules, which are composed of many atoms and are far more complex than spherical particles. From the systematic features in relation to N_{OH} , it can be inferred that the network structure of a hydrogen-bonding network, especially its topology, is essential for the glass transition. Therefore, molecules can be represented by network elements. From the similar probability of hydrogen bond formation, it is suggested that the connectivity between network elements is essentially identical for all polyhydric alcohols. Consequently, polyhydric alcohol can be regarded as a simple network system with a certain number of connective bonds per network element. According to this idea, we shall present a simple model that explains the temperature dependence of the structural relaxation time in the glass transition of polyhydric alcohols. Our purpose is to develop a coarse-grained model which provides a link between cooperative dynamics in supercooled liquids and microscopic structure. Although only hydrogen bonding liquids are considered in the present study, our approach presented here should be extended to other glass forming systems.

2. Overview of Model

On the basis of the above-mentioned experimental results, we focus on a hydrogen-bonding network to construct a model of the cooperative rearranging region (CRR) [11, 12]. In this model, a molecule is simplified as a node of the network and has a certain number of bonds that are connected or disconnected. A simplified molecule is referred to as a node, and a connecting bond represents a hydrogen bond between adjacent molecules. One OH group can form two hydrogen bonds because it can both donate a hydrogen atom to, and accept a hydrogen atom from, other OH groups. Therefore, maximum number of hydrogen bond per molecule is twice of number of OH groups in a molecule.

Experimental results suggest that the probability of hydrogen bond formation is insensitive to minor differences in the molecular structures of polyhydric alcohols, such as the position and number of OH groups and branching of the carbon chain [8, 9].

Therefore, we assume that the probability of forming a hydrogen bond follows a Boltzmann distribution with a certain value of binding free energy. Based on this free energy, the connectivity can be expressed as a function of temperature.

In our model, the CRR is regarded as a cluster in which molecules are connected through double hydrogen bonds. This assumption is based on the locally favored structures [13-15] inferred from local hydrogen bonding structure in the crystalline state [16-21]. As we have already defined the probability of hydrogen bond formation according to binding free energy, such clusters connected through double hydrogen bond can be treated mathematically.

To calculate the size of the cluster, we assume a Bethe lattice [22, 23] for the structure of the hydrogen-bonding network, where each node has a number of connective bonds, z . In this lattice, there is no pathway from one node back to itself (i.e., no loop structures). The connective probability p is equal to the probability of double hydrogen bond formation and therefore is given by the square of the probability of hydrogen bond formation p_b . One might question the validity this Bethe lattice assumption, since it appears to be physically unrealistic. However, it is known that when the cluster is sufficiently small, a Bethe lattice provides a good approximation of an actual lattice because the cluster is too small to include a loop structure. Furthermore, the Bethe lattice allows an exact solution to be found.

Thus, the estimated cluster of double hydrogen bonds in the Bethe lattice is identified as a CRR in reference to Adam-Gibbs theory [11]. From the size of the CRR, the relaxation time (τ) or frequency ($f = 1/2\pi\tau$) can be obtained. Because the cluster size depends on the connective probability, which is a function of temperature, the obtained relaxation time is dependent on temperature. With decreasing temperature, the

connective probability is increased, cluster size is increased, and consequently relaxation time is sharply increased.

3. Hydrogen Bond Formation

Experimental results have suggested that hydrogen bond formation is similar among a variety of polyhydric alcohols, regardless of minor differences in their molecular structures [8, 9]. Accordingly, we assume that hydrogen bond formation can be simply described by the binding free energy of hydrogen bonding.

Let the free energy of the bonded state and that of the non-bonded state be F_b and F_n , respectively. Then, $F_b = E_b - TS_b$ and $F_n = E_n - TS_n$, where E_b is the energy of the bonded state, S_b is the entropy of the bonded state, E_n is the energy of the non-bonded state, and S_n is the entropy of the non-bonded state. Assuming a Boltzmann distribution, the probability of bonded and non-bonded states is proportional to $\exp[-\beta F_b]$ and $\exp[-\beta F_n]$, respectively, where $\beta = 1/k_B T$ and k_B is the Boltzmann's constant. The normalized probability of hydrogen bond formation is given by $p_b = \exp[-\beta F_b] / (\exp[-\beta F_b] + \exp[-\beta F_n])$. Furthermore, p_b can be expressed as the difference in free energy between the bonded and non-bonded states:

$$p_b = 1 / (1 + \exp[-\beta \Delta F]), \quad (1)$$

where $\Delta F = F_n - F_b = \Delta E - T\Delta S$, $\Delta E = E_n - E_b$, and $\Delta S = S_n - S_b$.

To obtain these parameters, the coordination number is analyzed. Supposing that hydrogen bonds form independently from one another, the distribution function of coordination number $f(i)$ can be expressed by a binomial distribution function:

$$f(i) = {}_N C_i \cdot p_b^i (1 - p_b)^{N-i}, \quad (2)$$

where N is the maximum number of hydrogen bonds, $N = 2N_{OH}$, and i is the coordination number. Since p_b is a function of temperature, we have the coordination number distribution as a function of temperature with the parameter ΔF .

To confirm the validity of our assumption and to estimate the parameter ΔF (ΔE and ΔS), Eq. (1) is substituted into Eq. (2), and the result is compared with the coordination number reported by Chelli et al. from a molecular dynamics (MD) simulation on glycerol [16, 17]. In Fig. 1, the coordination number from their MD simulation is plotted against temperature. Solid curves in the figure show regression curves obtained by least-squares fitting using Eq. (2), where we have two free parameters (ΔE and ΔS) for all series of $f(0)$ - $f(6)$. For low-temperature data, it

was reported that the MD system did not reach equilibrium within the simulated timescale. Therefore, only the data above 270 K (at 394.9 K, 366.3 K, 319.4 K, and 278.1 K) were used in the fitting.

Despite having too many series of data ($f(0)$ - $f(6)$), good agreement is found among all the regression curves and MD data by using only two adjustable parameters ($\Delta E = 55.2$ meV (5.33 kJ/mol) and $\Delta S = 0.122$ meV/K (0.0118 kJ/mol K)). This result supports the validity of our simplified treatment of hydrogen-bonding connectivity.

Furthermore, from the same MD simulation reported by Chelli et al., the activation energy of hydrogen bond breaking was estimated to be 65 meV (6.3 kJ/mol) in the temperature range of 278-400 K ($1000/T = 2.5$ - 3.6 K⁻¹) [16, 17]. This activation energy should correspond to the hydrogen-bonding energy, ΔE . The values of ΔE from the coordination number distribution and that from the activation energy for hydrogen bond breaking agree within an error of 20%. These good agreements support the validity of our simplified treatment of hydrogen bonding.

4. Cluster Size in the Bethe Lattice

In the Section 5, the CRR will be treated as a cluster of double hydrogen bonds in a Bethe lattice. In this section, we shall briefly describe the Bethe lattice.

The schematic diagram of a Bethe lattice is shown in Fig. 2. Each site (solid circle) has a number of bonds, z . In the bond-percolation process, these bonds are connected with probability p , and disconnected with probability $1-p$. Since no loop structures appear in a Bethe lattice, exact solutions for several quantities can be easily obtained.

For the bond-percolation process, a cluster is defined as a set of sites that are connected by bonds. The mean cluster size S of a Bethe lattice is given exactly by the following equation [22, 23]:

$$S = (1 + p) / [1 - p(z - 1)]. \quad (3)$$

In a Bethe lattice, each branch is bifurcated infinitely, and the lattice extends infinitely. One might point out that such a lattice cannot exist within a realistic space. However, a Bethe lattice is still worth using for the following two reasons: firstly, the Bethe lattice is one of the few such models that allow an exact solution to be obtained; secondly, the Bethe lattice gives a good approximation of an actual lattice when the mean cluster size is sufficiently small. This is because the effect of loop structures is modest when the cluster size is small. Of course, for the systems of polyhydric alcohols considered in the present study, the Bethe lattice should no longer be valid around the critical point,

where the size of the cluster becomes infinite. As explained below, the critical point corresponds to the ideal glass transition point. Because this ideal point is experimentally inaccessible, the behavior around the critical point is beyond the scope of the proposed model.

5. Double Hydrogen Bonded Cluster

On the basis of Adam-Gibbs theory [11, 12], the structural relaxation is described as a cooperative thermally activated process. Consequently, the relaxation time is given by

$$f = f_0 \exp[-\beta n(T)\Delta\mu], \quad (4)$$

where $n(T)$ is the number of molecules incorporated into the CRR, $\Delta\mu$ is the activation energy for an independent process, f_0 is the relaxation frequency at the high temperature limit, and $f = 1/2\pi\tau$.

We assume that the CRR is a cluster composed of molecules linked by double hydrogen bonds. Recently, Tanaka and coworkers have pointed out that the density of locally favored structures formed between adjacent particles plays a key role in the glass transition [19-21]. Based on that finding, it is natural to consider the local structure found in the crystalline state. In the crystalline states of polyhydric alcohols, some adjacent molecules are connected by two or more hydrogen bonds [16-21]. If two molecules are connected by only one hydrogen bond, then each molecule can rotate about their torsional axis, and thus each molecule can undergo rearrangement (reorientation) independently. On the other hand, if they are connected by two hydrogen bonds, then the molecules cannot undergo rearrangement independently. Therefore, two or more hydrogen bonds are required for a rigid connection. In the disordered liquid phase, it is inferred that a hydrogen bond is formed according to a certain probability. If the hydrogen bonds are formed independently of one another, the probability of double hydrogen bond formation is the square of the probability of single hydrogen bond formation, the probability of triple hydrogen bond formation is the cube of the probability of single hydrogen bond formation, and so on. However, the probability of forming three or more hydrogen bonds is much less than that of forming two hydrogen bonds. Hence, we ignore the effects of three or more hydrogen bonds. Hence, if two molecules are connected by two hydrogen bonds, then they are included in the double hydrogen bonded cluster, and this cluster is associated with the CRR.

Independence of each hydrogen bond formation probability is just an approximation to enable us to obtain analytical solution. In actual system, effects of steric hindrance and

position of OH group might appear. However, experimental results has clearly shown that T_g and fragility are insensitive of minor differences in molecular structures [8, 9].

Furthermore, analysis on orientational correlation factor regarding OH groups suggests that hydrogen bond formation and its temperature dependence are also insensitive of molecular structure of polyhydric alcohols [8, 9]. These experimental results support the validity of our approximation on independent hydrogen bonds formation. In addition, we have presented the analysis on coordination number based on the independent hydrogen bond formation in section 3. This analysis successfully reproduces the complicated data reported form MD simulation. Therefore, this approximation is applicable at least as a primary step to develop a model of the CRR.

To evaluate the size of the double hydrogen bonded cluster, we consider the bond-percolation process in the Bethe lattice. Here, molecules are represented as nodes on the Bethe lattice, and double hydrogen bonds are represented by a connected bond. Since each OH group is capable of forming two hydrogen bonds as both a hydrogen donor and acceptor, the maximum number of single hydrogen bonds for each molecule is twice as number of OH group per molecule (N_{OH}). Since maximum number of double hydrogen bonds is half of that of single hydrogen bonds, the maximum number of double hydrogen bonds is N_{OH} . Therefore, the number of bonds, z , in our Bethe lattice should be equal to N_{OH} ($z = N_{OH}$). The connection probability p in our Bethe lattice is equal to the probability of a double hydrogen bond formation ($p = p_b^2$). Thus, recalling Eqs. (3) and (1), we can express the size of the double hydrogen bonded cluster as

$$\begin{aligned}
 S &= (1 + p_b^2) / [1 - p_b^2(N_{OH} - 1)] \\
 &= \frac{(1 + \exp[-\beta\Delta F])^2 + 1}{(1 + \exp[-\beta\Delta F])^2 - (N_{OH} - 1)} \\
 &= \frac{(1 + \exp[\Delta S/k_B - \Delta E/k_B T])^2 + 1}{(1 + \exp[\Delta S/k_B - \Delta E/k_B T])^2 - (N_{OH} - 1)}. \tag{5}
 \end{aligned}$$

Then, this cluster is associated with the CRR ($n(T) = S$), and substituting Eq. (5) into Eq. (4), we have the relaxation frequency:

$$f = f_0 \exp \left[\frac{\Delta\mu}{k_B T} \cdot \frac{(1 + \exp[\Delta S/k_B - \Delta E/k_B T])^2 + 1}{(1 + \exp[\Delta S/k_B - \Delta E/k_B T])^2 - (N_{OH} - 1)} \right]. \quad (6)$$

Thus, the relaxation frequency f is a function of temperature. Here, the size of the CRR, and consequently the relaxation frequency, exhibit divergence at a certain temperature due to the critical property of the Bethe lattice. Around the critical point, the size of the CRR increases sharply, and then the hydrogen-bonding network can no longer be regarded as a Bethe lattice. However, we are not interested in this critical point, because it is experimentally inaccessible due to the very long relaxation time.

6. Comparison between Theoretical and Experimental Results

To evaluate the validity of our model, experimentally obtained the relaxation frequencies of several polyhydric alcohols [6-9] are fitted using Eq. (6), where the free parameters are ΔE , ΔS , $\Delta\mu$, and f_0 (the hydrogen-bonding energy, hydrogen-bonding entropy, independent activation energy, and high-temperature limit of relaxation frequency). The results of the fitting are shown in Fig. 3. Clearly, all the experimental data are reproduced well by Eq. (6) with reasonable values of the parameters ΔE , ΔS , $\Delta\mu$, and f_0 . Although this Eq. (6) has more free-parameters than conventionally used Vogel-Fulcher-Tammann (VFT) equation [24-26], the qualities of each fit are practically the same. However, now physical picture of each parameter of Eq (6) is clear whereas essentially no physical picture has been presented for the parameters of VFT equation. In addition, VFT equation can be derived from it as to be shown in the next section.

In Fig. 4, these obtained parameters, except for f_0 , are plotted against N_{OH} , and also listed in the table. As can be seen in this figure, the obtained values of ΔE , ΔS , and $\Delta\mu$ are approximately the same for all polyhydric alcohols examined here. The mean values of ΔE , ΔS , and $\Delta\mu$ are 35.1 meV, 0.169 meV/K, and 208 meV (3.39 kJ/mol, 0.0163 kJ/mol K, and 20.1 kJ/mol), respectively; and the standard deviations are 4.2 meV, 0.016 meV/K, and 13 meV, respectively (12%, 9.6%, and 6.1% of each mean value). From this analysis, it can be concluded that the obtained values of these parameters are highly similar among a variety of polyhydric alcohols.

The similarity in the obtained values of ΔE and ΔS can be attributed to the similarity in the formation of hydrogen bonds. In previous works on polyhydric alcohols based on the analysis of orientational correlation factor via the dielectric constant, it

has been suggested that the formation of hydrogen bonds is similar among all polyhydric alcohols, irrespective of differences in their molecular structures [8, 9]. On the basis of this finding, we have constructed the present model. Therefore, the similarity found in the values of ΔE and ΔS supports the validity of our model. Furthermore, the values of ΔE and ΔS are the same magnitude as the values calculated from the coordination number distribution from MD data in Section 3. These values are plotted as open triangles in Fig. 4 (a) and (b). Although these values show slight differences, the magnitude is of the same order. Since our model is schematic and includes some approximation, this degree of agreement is remarkable. Since we completely neglect the effect of molecular structure, such as steric requirement of hydrogen bonding and intra-molecule hydrogen bonding, this deviation can be attributed to these effects. It is expected that this deviation can be compensated by taking into account actual probability of inter-molecular hydrogen bonding.

Although we did not specify a physical description of independent motion, the obtained value of $\Delta\mu$ is nonetheless found to be physically plausible. The values of $\Delta\mu$ in our model are comparable with the activation energy of a configurational change, specifically, the energy barrier of a gauche-trans (g-t) conformational change. For example, it has been reported from MD simulations on glycerol that the mean g-t activation energy is 209 meV (20.2 kJ/mol) [16, 17]. In addition, the barrier height of the g-t conformational change of ethane is known to be 120 meV (12 kJ/mol) from calorimetric measurement [27]. These two values are plotted in Fig. 4 (c) as open diamonds and squares, respectively. From this result, it is inferred that a type of g-t conformational change is responsible for the fundamental process of structural relaxation. These agreements of obtained value of $\Delta\mu$ with g-t activation energy, further support validity of our model.

The size of the CRR, defined as the number of nodes incorporated in the cluster, is next calculated using Eq. (5) with the obtained parameters. The temperature dependence of the size of the CRR is plotted against reciprocal temperature in Fig. 5. As shown in this figure, the size of the CRR increases with decreasing temperature. These results show that 2-5 molecules are incorporated into the CRR at T_g , and these values are consistent with other reports. For several glass-forming materials, Yamamuro and coworkers used configurational entropy, obtained from the specific heat in liquid and crystalline phases, to estimate the size of the CRR [28, 29]. The reported CRR size is in the range of 3-8 at T_g , and the magnitude of these values is comparable with our result.

Since the Bethe lattice approximation is valid when the size of cluster is sufficiently small (roughly within the number of adjacent nodes), our Bethe lattice approximation is supported by the calculated cluster size.

7. Lower-Bound Free Energy Approximation

By taking the lower limit of free energy, our model yields the VFT equation. The validity of this approximation is to be presented after derivation of the VFT equation.

Assuming $|\beta\Delta F| \ll 1$, the approximate probability of hydrogen bond formation is

$$p_b = \frac{1}{1 + \exp(-\Delta F/k_B T)} \cong \frac{1}{2} \left(1 - \frac{1}{2} \Delta F/k_B T \right)^{-1}. \quad (7)$$

Squaring each side of this equation and again taking the lower limit of free energy, we have the probability of double hydrogen bond formation:

$$p_b^2 = \frac{1}{4} \left(1 - \frac{1}{2} \Delta F/k_B T \right)^{-2} \cong \frac{1}{4} (1 + \Delta F/k_B T). \quad (8)$$

Substituting Eq. (8) into Eq. (5), the size of the CRR is expressed as follows,

$$S \cong \frac{5T(1 + \Delta F/5k_B T)}{(5 - \Delta S/k_B) + (\Delta S/k_B - 1)N_{OH}} \cdot \frac{1}{T - T_0}, \quad (9)$$

where $T_0 = (N_{OH} - 1)(\Delta E/k_B) / [(5 - \Delta S/k_B) + (\Delta S/k_B - 1)N_{OH}]$. Here, again invoking $|\Delta F/k_B T| \ll 1$,

$$S \cong \frac{5T}{(5 - \Delta S/k_B) + (\Delta S/k_B - 1)N_{OH}} \cdot \frac{1}{T - T_0}. \quad (10)$$

Similar to the derivation of Eq. (6), when Eq. (10) is substituted into Eq. (4), it follows that

$$\begin{aligned} f &= f_0 \exp \left[- \frac{\Delta\mu}{k_B T} \cdot \frac{5T}{(5 - \Delta S/k_B) + (\Delta S/k_B - 1)N_{OH}} \cdot \frac{1}{T - T_0} \right] \\ &= f_0 \exp \left[- \frac{B}{T - T_0} \right], \end{aligned} \quad (11)$$

where $B = 5(\Delta\mu/k_B) / [(5 - \Delta S/k_B) + (\Delta S/k_B - 1)N_{OH}]$. Thus, VFT equation has been

derived under the lower-bound free energy approximation.

Invoking the definitions of the fragility index and glass transition temperature, these quantities are expressed as functions of N_{OH} :

$$m = - \left. \frac{d \log f}{d(T_g/T)} \right|_{T=T_g} = \frac{T_0}{B} \cdot \frac{(\log f_0/f_g)^2}{\log e} + \log f_0/f_g$$

$$= \frac{(N_{OH} - 1)\Delta E}{5\Delta\mu} \cdot \frac{(\log f_0/f_g)^2}{\log e} + \log f_0/f_g, \quad (12)$$

and

$$T_g = T_0 + \frac{B \log e}{\log f_0/f_g}$$

$$= \frac{1}{(5 - \Delta S/k_B) + (\Delta S/k_B - 1)N_{OH}} \left[(N_{OH} - 1)\Delta E/k_B + \frac{5\Delta\mu \log e}{k_B \log f_0/f_g} \right].$$

(13)

Here, f_g is defined as the frequency at the glass transition temperature (here,

$$f_g = 10^{-2} \text{ Hz}).$$

To confirm the applicability of our lower-bound free energy approximation, this condition should be analyzed in detail. The lower-bound free energy condition,

$$-1 \ll \Delta F/k_B T \ll 1, \text{ can be rewritten as}$$

$$\frac{(\Delta E/k_B)/[\Delta S/k_B + 1] \ll T \ll (\Delta E/k_B)/[\Delta S/k_B - 1]. \quad (14)$$

Therefore, the approximation result, Eq. (11), should be employed only within this temperature range. To confirm this, $T_{lwb} = (\Delta E/k_B)/[\Delta S/k_B + 1]$,

$T_{upb} = (\Delta E/k_B)/[\Delta S/k_B - 1]$, and T_g for all examined materials are listed in Table 1.

Clearly, the values of T_g are within the range from T_{lwb} to T_{upb} . Therefore, this

approximation is applicable around T_g . Moreover, the experimental temperature range

for the reported data, 193 - 363 K, is entirely within this applicable temperature range.

In order to compare the approximation with experimental results, the parameters T_g and T_0 , and m are plotted against N_{OH} in Figs. 6 and 7, respectively. For the

theoretical curves, $\log f_0 = 14.05$, $\Delta E = 31.6$ meV, $\Delta S = 0.157$ meV/K, and $\Delta\mu = 216$ meV ($\Delta E = 3.05$ kJ/mol, $\Delta S = 0.0152$ kJ/molK, and $\Delta\mu = 20.9$ kJ/mol) were employed, where these values were averaged for a set of sugar alcohols. From Figs. 6 and 7, it can be seen that the values of T_g , T_0 , and m agree well between theory and experiment. In particular, the agreement for sugar alcohols is excellent. Since these quantities are often used to characterize the slow dynamics around T_g , our model successfully describes the slow dynamics. It should be noted that experimental values of T_g , T_0 , and m slightly depend on N_C and molecular structure. Such slight molecular structure dependence is not taken into account in our model. Therefore, this may cause a slight discrepancy between the experimental and theoretical values, as seen in the values for $N_{OH} = 3$ in Figs. 6 and 7.

To make a comparison between theory and experiment at lower N_{OH} , the VFT parameters of ethylene glycol (EG; a sugar alcohol with $N_{OH} = 2$) are discussed. However, pure EG in a supercooled state has a high tendency to crystallize. Therefore, precise VFT parameters are not available. For this reason, the data on mixtures of EG and water are employed here. A water molecule has two hydrogen atoms, and therefore has two hydrogen donors. Accordingly, it is presumed that a water molecule (H-O-H) consists of two OH groups, although the oxygen atoms in both OH groups are identical. Thus, N_{OH} of water is 2. Since N_{OH} of both EG and water is 2, N_{OH} of the mixture is also regarded as 2, independent of the mixing ratio. The data on EG and water mixtures, as measured by dielectric spectroscopy [30], are plotted in Figs. 6 and 7 as open symbols. From these figures, it can be seen that the experimental values of T_g , T_0 , and m are in good agreement with the theoretical values until $N_{OH} = 2$.

Despite the simplicity of our model, it can sufficiently explain the experimentally obtained characteristic of slow dynamics. The agreement for the data on sugar alcohols is especially surprising. From these results, the validity of our model is strongly supported.

In the present paper, only hydrogen-bonding liquids are considered, but a similar approach should be applicable to other networks of glass-forming materials, such as covalent glass. For such extension of the model, the present double hydrogen bonded cluster should be replaced by system-specific clusters. For covalent glasses, the characteristic local structure of short-range motifs, so-called medium-range order [31],

may correspond to the double hydrogen bonds considered here. For example, Wilson et al. have conducted a computer simulation on SiO_2 -based glasses, and found that differences in the connectivity of SiO_2 tetrahedral motifs are linked to fragility [32]. In fact, similar systematic features in T_g and fragility have also been reported for such inorganic glasses [33-36]. Although the alternative structure for the double hydrogen bond is still unclear for other systems, shedding light on this type of structure should give a new physical picture of the CRR based on more general perspectives.

8. Conclusion

We have developed a new model that explains the glass transition of polyhydric alcohols on the basis of percolation process of a network of double hydrogen bonds. The temperature dependence of the relaxation time for reported polyhydric alcohols (sugar alcohols and trihydric alcohols) were reproduced well by our model. In addition, the calculated values of parameters agree with microscopic quantities obtained by simulation and experiment. By considering the lower-bound approximation of binding free energy in the present theory, the VFT equation was derived. Thus, we obtained an analytical expression for the glass transition temperature, fragility, and VFT parameters as a function of the number of OH in a molecule (N_{OH}). These quantities were found to depend on N_{OH} , in good agreement with reported experimental results for polyhydric alcohols including water-sugar alcohol mixtures.

9. Acknowledgements

We thank Professor K. Nemoto for valuable discussions and advice. This work was supported by the Clark Memorial Foundation of Hokkaido University.

References

- [1] G. E. Gibson, W. F. Giauque, *J. Am. Chem. Soc.* **45**, 93 (1923).
- [2] U. Schneider, P. Lunkenheimer, R. Brand, A. Loidl, *J. Non-Cryst. Solids* **235-237**, 173 (1998).
- [3] A. Döb, M. Paluch, H. Sillescu, G. Hinze, *Phys. Rev. Lett.* **88**, 095701 (2002).
- [4] A. Döb, M. Paluch, H. Sillescu, G. Hinze, *J. Chem. Phys.* **117**, 6582 (2002).
- [5] K. L. Ngai, M. Paluch, *J. Phys. Chem. B* **107**, 6865 (2003).
- [6] A. Minoguchi, K. Kitai, R. Nozaki, *Phys. Rev. E* **68**, 031501 (2003).
- [7] A. Minoguchi, T. Kaneko, H. Sotokawa, R. Nozaki, *J. Non-Cryst. Solid.* **352**, 4742 (2006).
- [8] M. Nakanishi, R. Nozaki, *Phys. Rev. E* **81**, 041501 (2010)
- [9] M. Nakanishi, R. Nozaki, *Phys. Rev. E* **83**, 051503 (2011)
- [10] C. A. Angell, *J. Non-Cryst. Solids* **131-133**, 13 (1991).
- [11] G. Adam, J. H. Gibbs, *J. Chem. Phys.* **43**, 139 (1965).
- [12] K. Binder, W. Kob, *Glassy Materials and Disordered Solids* (World Scientific Publishing Co. Pte. Ltd., Singapore, 2005)
- [13] H. Tanaka, *J. Non-Cryst. Solids* **351**, 3371 (2005).
- [14] C. P. Royall, S. R. Williams, T. Ohtsuka, H. Tanaka, *Nature Materials* **7**, 556 (2008)
- [15] K. Watanabe, H. Tanaka, *Phys. Rev. Lett.* **100**, 158002 (2008).
- [16] R. Chelli, P. Procacci, G. Cardini, R. G. D. Valle, S. Califano, *Phys. Chem. Chem. Phys.* **1**, 871 (1999).
- [17] R. Chelli, P. Procacci, G. Cardini, S. Califano, *Phys. Chem. Chem. Phys.* **1**, 879 (1999).
- [18] H. M. Berman, G.A. Jeffrey, R.D. Rosenstein, *Acta Cryst. B* **24**, 442 (1968).
- [19] H. S. Kim, G. A. Jeffrey, *Acta Cryst. B* **25**, 2607 (1969).
- [20] N. Azarnia, G. A. Jeffrey, M. S. Shena, *Acta Cryst. B* **28**, 1007 (1972).
- [21] M. Rukiah, J. Lefebvre, O. Hernandez, W. Beek, M. Serpelloni, *J. Appl. Cryst.* **37**, 766 (2004).
- [22] D. Stauffer, A. Aharony, *Introduction to Percolation Theory* 2nd Ed., Taylor & Francis, London (1994).
- [23] M. E. Fisher, J. W. Essam, *J. Math. Phys.* **2**, 609 (1961).
- [24] H. Vogel, *Phys. Z.* **22**, 645 (1921).
- [25] G. S. Fulcher, *J. Am. Ceram. Soc.* **8**, 339 (1925).
- [26] G. Tammann, W. Hesse, *Anorg. Allg. Chem.* **156**, 245 (1926).
- [27] G. Stroble, *The Physics of Polymers* 2nd Ed., Springer, Berlin Heidelberg New York, (2002)

- [28] S. Takahara, O. Yamamuro, T. Matsuo, *J. Phys. Chem.* 99, 9589 (1995).
- [29] O. Yamamuro, I. Tsukushi, A. Lindqvist, S. Takahara, M. Ishikawa, T. Matsuo, *J. Phys. Chem. B*, 102, 1605 (1998).
- [30] S. Sudo, N. Shinyashiki, S. Yagihara, *J. Mol. Liq.* 90, 113 (2001).
- [31] S. R. Elliott, *Nature* 354, 445 (1991).
- [32] M. Wilson, P. S. Salmon, *Phys. Rev. Lett.* 103, 157801 (2009).
- [33] M. Tatsumisago, B. L. Halfpap, J. L. Green, S. M. Lindsay, C. A. Angell, *Phys. Rev. Lett.* 64, 1549 (1990).
- [34] R. Böhmer, C. A. Angell, *Phys. Rev. B*, 45, 10091 (1992).
- [35] G. D. Chryssikos, J. A. Duffy, J. M. Hutchinson, M. D. Ingram, E. I. Kamitsos, A. J. Pappin, *J. Non-Cryst. Solid.* 172-174, 378 (1994).
- [36] S. Kojima, V. N. Novikov, M. Kodama, *J. Chem. Phys.*, 113, 6344 (2000).

Table

Table 1. List of the obtained parameters for Eq. (6) and the temperature range where low free energy approximation is applicable. This approximation is applicable under the

condition $T_{lwb} \ll T \ll T_{upb}$, where $T_{lwb} = (\Delta E / k_B) / [\Delta S / k_B + 1]$,

$$T_{upb} = (\Delta E / k_B) / [\Delta S / k_B - 1].$$

Sample	N_{OH}	ΔE (meV)	ΔS (meV/K)	$\Delta\mu$ (meV)	$n(T_g)$	m	T_0 (K)	T_{lwb} (K)	T_g (K)	T_{upb} (K)
Sorbitol	6	32.7	1.89	198	4.3	102.2	229	131	268	427
Xylitol	5	31.0	1.80	213	3.7	78.3	198	129	248	450
Threitol	4	32.7	1.86	225	3.2	68.4	175	133	226	442
Glycerol	3	29.7	1.75	229	2.7	50.0	129	125	192	460
Butanetriol	3	37.1	2.00	196	3.0	60.7	153	143	201	430
3MPT ^a	3	36.0	1.90	207	3.0	57.0	152	144	206	464
Hexanetriol	3	40.2	2.18	196	3.0	67.6	161	147	202	395
Heptanetriol	3	41.2	2.29	206	2.8	68.2	161	145	200	371

^a 3-Methyl-1,3,5-pentanetriol

Figure Captions

Fig. 1. Distribution function of coordination number against temperature. Symbols represent MD simulation data [16, 17], and solid curves show the result of least-squares fitting using Eq. (1) substituted into Eq. (2).

Fig. 2. Schematic of Bethe lattice. Solid circles represent nodes. Solid and dotted lines stand for connected and disconnected bonds, respectively. This figure is an example of $z = 3$.

Fig. 3. Arrhenius diagram of relaxation frequency for polyhydric alcohols. Symbols show previously reported data [6-9]. Solid curves show fitting using Eq. (6).

Fig. 4. Parameters in Eq. (6): (a) binding energy, (b) entropy, and (c) independent activation energy. Solid circles are obtained from the fitting shown in Fig. 2. Open triangles show binding energy and entropy from Fig. 1. Open diamonds show the reported energy barrier of the gauche-trans conformational change of glycerol [16, 17]. Open squares show the energy barrier of the gauche-trans conformational change of ethane [24].

Fig. 5. Temperature dependence of CRR size, calculated using Eq. (5). Solid curves show CRR size for materials shown in Fig. 3. Symbols on each curve show the values of CRR size at T_g , and each symbol match to that used in Fig. 3. The values of size of CRR at T_g are also listed in the table.

Fig. 6. Glass transition temperature T_g and Vogel temperature T_0 against N_{OH} . Solid curves show theoretical values from our model presented in Section 7. Solid symbols show experimental values from references [6-9]. Open symbols show the values for EG-water mixtures (60, 70, and 80 wt %) [30]. Values of T_g and T_0 are also listed in the table.

Fig. 7. Fragility index m against N_{OH} . Solid curve shows theoretical value from our model presented in Section 7. Solid symbols show experimental value from references

[6-9]. Open symbols show the values for EG/water mixtures (60, 70, and 80 wt %) [30].

Values of T_g and T_0 are also listed in the table.

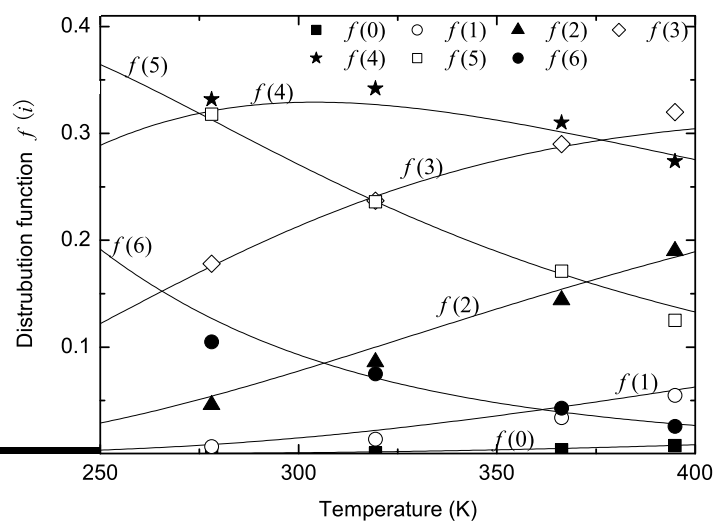


Figure 1 ED10766 06JUN2011

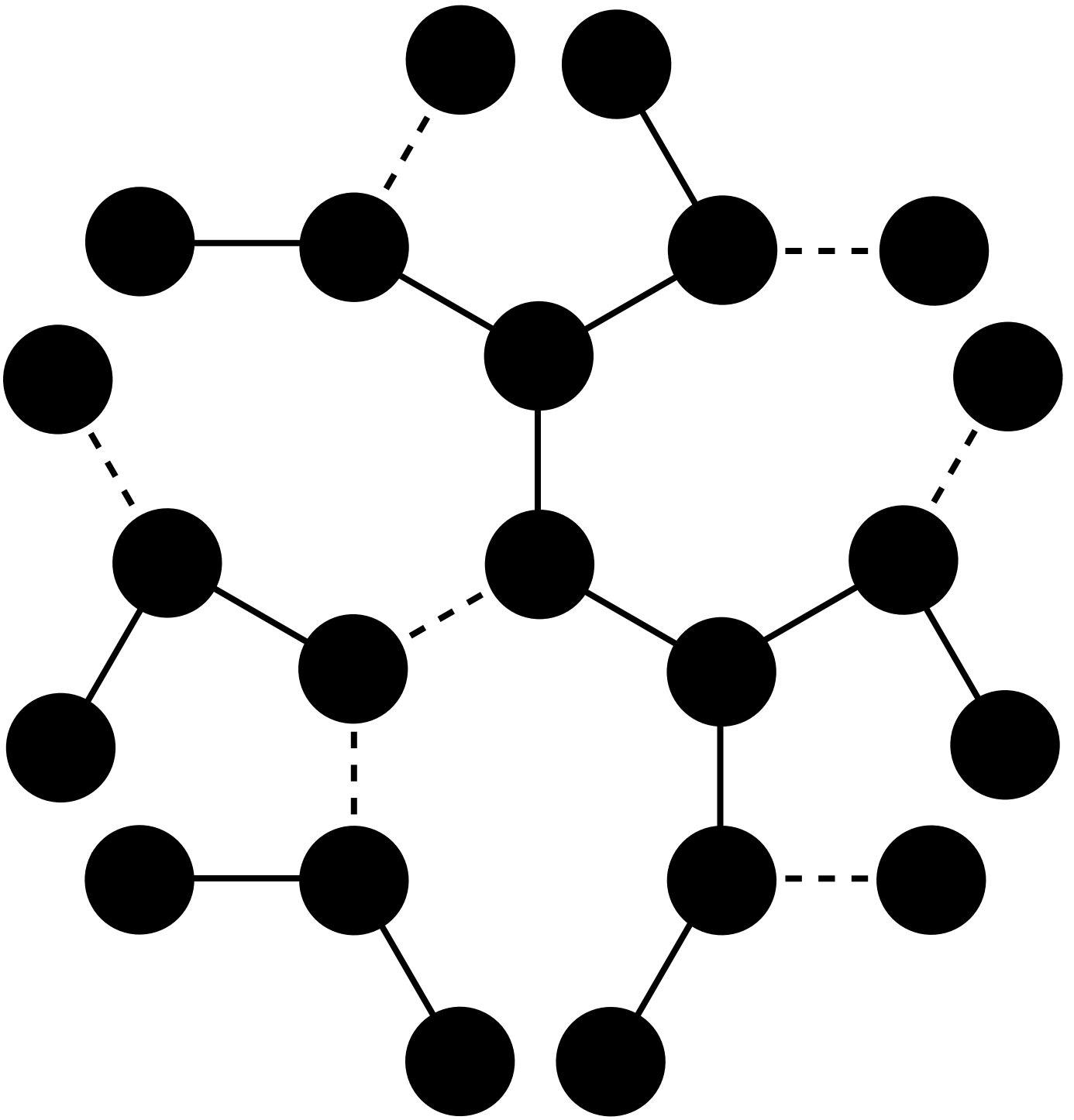


Figure 2

ED10766

06JUN2011

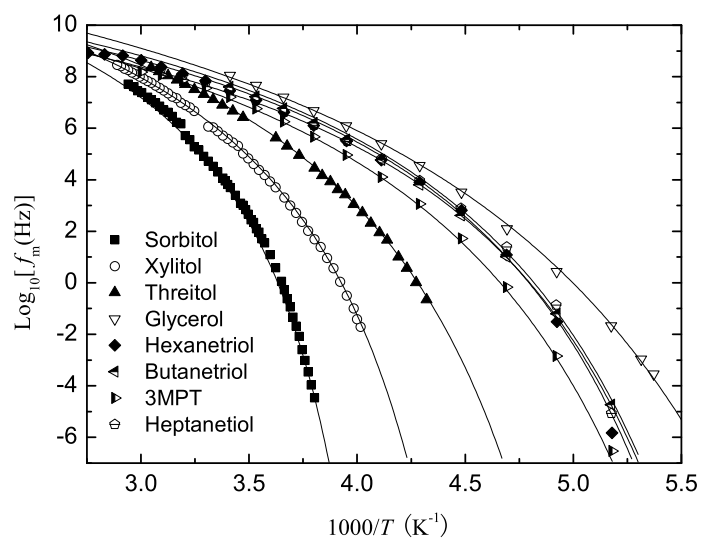


Figure 3

ED10766

06JUN2011

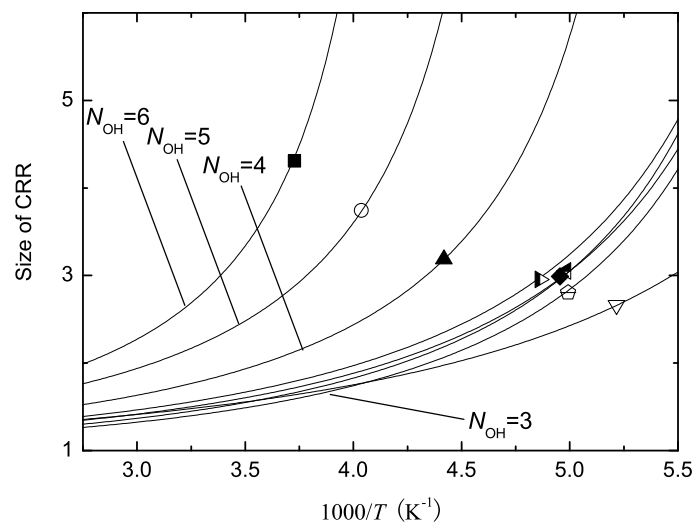


Figure 5 ED10766 06JUN2011

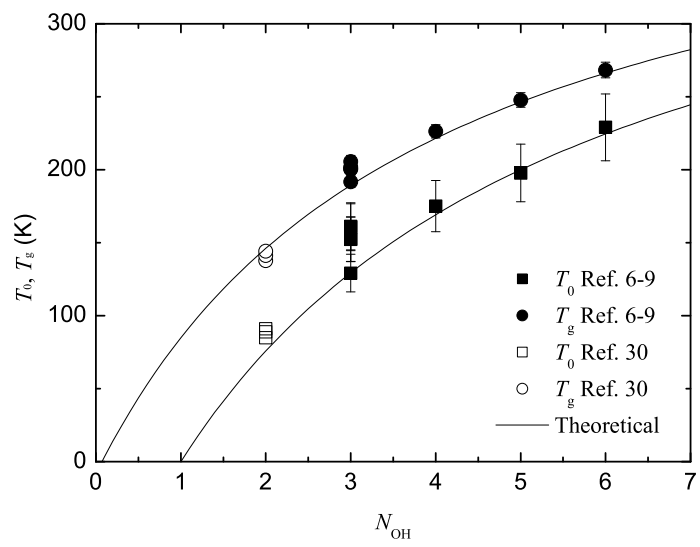


Figure 6

ED10766

06JUN2011

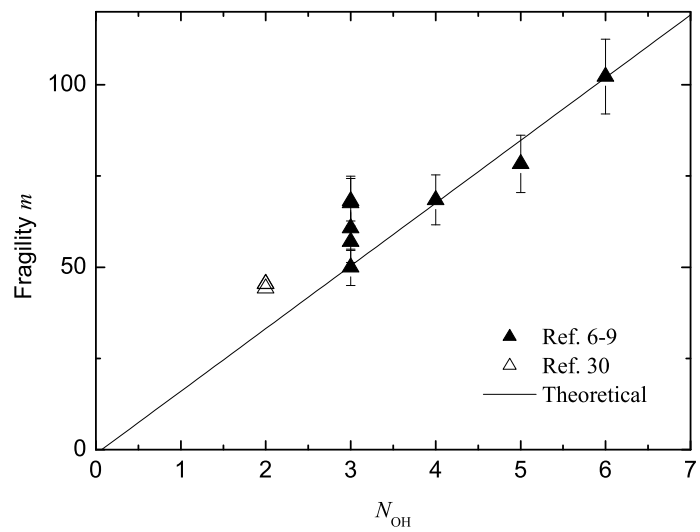


Figure 7 ED10766 06JUN2011